Inorganic Chemistry

Article

pubs.acs.org/IC

Luminescent Properties of Metal–Organic Framework MOF-5: Relativistic Time-Dependent Density Functional Theory Investigations

Min Ji, Xin Lan, Zhenping Han, Ce Hao,* and Jieshan Qiu

State Key Laboratory of Fine Chemicals, School of Chemical Engineering, Dalian University of Technology, Dalian 116024, Liaoning, China

ABSTRACT: The electronically excited state and luminescence property of metal–organic framework MOF-5 were investigated using relativistic density functional theory (DFT) and time-dependent DFT (TDDFT). The geometry, IR spectra, and UV–vis spectra of MOF-5 in the ground state were calculated using relativistic DFT, leading to good agreement between the experimental and theoretical results. The frontier molecular orbitals and electronic configuration indicated that the luminescence mechanism in MOF-5 follows ligand-to-ligand charge transfer (LLCT), namely, $\pi^* \rightarrow \pi$, rather than emission with the ZnO quantum dot (QD) proposed by Bordiga et al. The geometry and IR spectra of MOF-5 in the electronically excited state have been calculated using the relativistic TDDFT and compared with those for the ground state. The comparison reveals that the Zn_4O_{13} QD is rigid, whereas the ligands BDC^{2-} are nonrigid. In addition, the calculated emission band of MOF-5 is in good agreement with the experimental result and is similar to that of the ligand H_2BDC. The combined results confirmed that the luminescence mechanism for MOF-5 should be LLCT with little mixing of the ligand-to-metal charge transfer. The reason for the MOF-5 luminescence is explained by the excellent coplanarity between the six-membered ring consisting of zinc, oxygen, carbon, and the benzene ring.

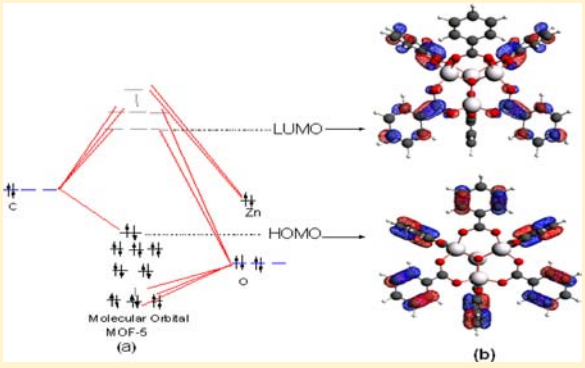

INTRODUCTION

Metal–organic frameworks (MOFs) have emerged as an extensive class of nanoporous materials. These are crystalline hybrid inorganic/organic solids with structures that are composed of clusters of a few metal atoms held together in a three-dimensional structure by organic linkers. The MOFs have attracted great interest because of their diverse properties and highly tunable construction. Numerous uses have been investigated, including gas storage/separations, optics, molecule recognition, and electronics.[1−5] The first reports of luminescence in structures called "MOF", that we are aware of, appeared in 2002. By March 2011, nearly 1337 articles have appeared reporting MOF light emissions and a few reviews covering certain aspects of the MOF luminescence properties have been published.[6] The new type of organic–inorganic hybrid materials is certainly very promising as a multifunctional luminescent material because both the inorganic and organic moieties can provide platforms to generate luminescence; meanwhile, metal–ligand charge-transfer-related luminescence within MOFs can add another dimension to the luminescence functionality.[7−9] Therefore, MOFs have various modes for generating luminescence, including MLCT, LMCT, LLCT, MMCT, etc. (M = metal, L = ligand, and CT = charge transfer).[10,11] Furthermore, some guest molecules within MOFs can also emit and/or induce luminescence.[12] Currently, MOFs are considered as materials with great potential and with possible industrial applications such as, for example, luminescent materials,[13] sensors,[14] and photocatalysts.[15]

With numerous unique properties, MOF-5, which was invented by Yaghi and co-workers[16] in 1999, has become one of the more promising MOFs. A high capacity for hydrogen storage[17,18] and luminescence are just two properties.[19−23] Within the huge MOF family of structures, the most well-known is probably MOF-5, which is the first member of a series of isoreticular MOFs with oxide-centered Zn_4O tetrahedra as nodes, or quantum dots (QDs), linked by organic molecules. Thus, the behavior of ZnO QDs within MOF-5 contributes considerably to luminescence. The ZnO QD absorption and emission spectra from electronic transitions have been investigated by Bordiga et al.[19] They guessed that the luminescent behavior of MOF-5 arises from a $O^{2-}Zn^{+} \rightarrow O^{-}Zn^{+}$ charge-transfer transition within each tetrahedral Zn_4O_{13} metal cluster, which has been described as a ZnO-like QD. The peak intensity of photoluminescence emissions of MOF-5, observed at 525 nm, was ascribed to energy harvesting and LMCT from 1,4-benzenedicarboxylate (BDC^{2-}) linked to the Zn_4O_{13} cluster. The nature of the luminescence transitions in MOF-5 nanoparticles has been investigated by Tachikawa et al.[20] Basically, the transition responsible for the green emission

Received: August 13, 2012
Published: November 8, 2012

   dx.doi.org/10.1021/ic301771b | *Inorg. Chem.* 2012, 51, 12389–12394

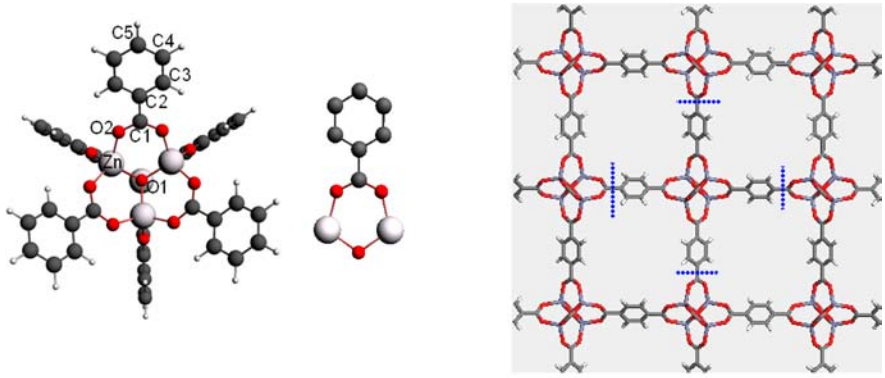

Figure 1. (a) Representative fragment of the MOF-5 structure with atomic labels as used in the text. (b) Coplanar structure. (c) Detail that the MOF-5 crystal structure is truncated into a representative segment (blue dashed lines: the clipping position).

of MOF-5 is similar to that of ZnO. Therefore, the emission observed in MOF-5 has been proposed to originate from the ZnO QD.

The luminescent properties of nanoscale ZnO impurities existing in MOF-5 and highly pure MOF-5 have been investigated by Feng et al.[21] Upon excitation at 365 nm, the former exhibits an intense luminescence at 535 nm, which was similar to the results previously reported by Bordiga and Tachikawa. Upon excitation at 345 nm, the latter exhibits a single emission at 397 nm; the ligand H_2BDC emission was at 382 nm. The similarities between the pure MOF-5 and ligand H_2BDC emission spectra indicate a link-centered emission for MOF-5 free of LMCT. By considering the effects of quantum confinement, they thought that the particle-size distribution of these ZnO particles may be estimated from the excitation and absorption spectra, leading to size-dependent shifts in the absorbance and excitation spectra. For this reason, the MOF-5 emissions have been considered to be luminescence from ZnO QDs.

Thus, the behavior of the ZnO-like QD or ligand in the electronically excited state has not been researched to any great extent, least of all to the extent of its influence on luminescence. The problem needs a quantum chemical calculation to be resolved. At present, time-resolved ultrafast spectroscopy, quantum chemical calculations for excited states, and excited-state dynamics simulations have been versatile tools in studying the electronic excited-state ultrafast dynamics of complex molecular systems.[24,25] Combining time-resolved spectroscopic experiments with excited-state quantum chemical calculations and dynamics simulations has proven to be valuable.[26] Especially, density functional theory (DFT) and time-dependent DFT (TDDFT) were widely used to study the excited-state behaviors of molecules and supramolecules.[27−29] In this study, we used relativistic DFT and TDDFT to investigate luminescence in MOF-5. Frontier molecular orbitals (MOs) and the electronic configuration were used to analyze the underlying mechanism. We demonstrated the relationship between the luminescence behavior of a ZnO-like QD and ligand H_2BDC by comparing IR spectra, bond order and emission spectra of the ground state, and the electronically excited states.

COMPUTATION DETAILS

As reported in the literature, calculation of the chemical properties of MOF-5 using a representative fragment is in good agreement with the experimental results.[30−32] In the crystal structure of MOF-5, every Zn_4O cluster is coordinated by six 1,4-benzenedicarboxylate (BDC) groups. In this paper, thus, we clipped a carboxylate of BDC and thereby truncated the MOF-5 crystal structure into a representative segment, consisting of one Zn_4O cluster and six BDC groups (Figure 1). Meanwhile, we labeled a number of different types of atoms in the figure. The ground-state geometric optimization was performed by using the relativistic DFT method with generalized gradient approximation of Becker's exchange functional and the Lee−Yang−Parr gradient-corrected correlation functional (BLYP).[33−35] The excited-state electronic structures were calculated using the relativistic TDDFT method with the BLYP functional. A higher self-consistent-field convergence standard of 10^{-8} was used in the ground- and excited-state geometry optimization. The excited-state IR spectra, bond length, and bond order were calculated using the optimized excited-state structures, and the integration accuracy is 5.0. For all of the calculated structures, the triple-ζ plus polarization basis set was chosen.[36] The relativistic effects have an important impact for the heavy elements in the molecular theory calculation.[37,38] Therefore, we employ the zero-order approximation method for the all-electron scalar relativistic DFT calculations.[39−41] The relativistic method was found to be reliable.[42] Besides, the exchange-correlation functional is also proven to be crucial for the optoelectronic properties of metal-containing molecules.[43,44] Especially, the Hirao group[45] has shown that long-range-corrected (LC)-TDDFT incorporating relativistic effects is one of the best methods for the excited-state calculation of light systems. However, for large systems like MOF-5, the relativistic LC-TDDFT with a Hartree−Fock exchange effect is limited because of the quality of the short-range exchange functional and the speed of computation.[45] Thus, the calculation did not consider the influence of the Hartree−Fock exchange effect on the excited-state properties of MOF-5. All of the calculations are carried out with the Amsterdam Density Functional program package.[46,47] The calculated spectra (including IR, absorption, and emission spectra) used the Gaussian line shape.

RESULTS AND DISCUSSION

Ground-State Geometric Conformations. In the MOF-5 fragment, the central and peripheral oxygen atoms formed two kinds of coordination bonds, O1−Zn and O2−Zn, with metal zinc, respectively. The ligands BDC^{2-} were classified as C1−O2, C1−C2, C2−C3, C3−C4, and C4−C5 bonds. We used the relativistic DFT method to optimize the ground-state geometric conformations of the MOF-5 fragment. The fully optimized conformation is shown in Figure 1a. Comparisons of the calculated bond lengths and dihedral angles with reported values are listed in Table 1. After a careful comparison, we have found that our calculated results are consistent with the

dx.doi.org/10.1021/ic301771b | Inorg. Chem. 2012, 51, 12389−12394

Table 1. Calculated and Experimental Geometric Parameters for the MOF-5 Fragment in the Ground State

	exptl[32]	this work
	Bond Length (Å)	
O1−Zn	1.968	1.978
Zn−O2	1.947	1.987
O2−C1	1.254	1.284
C1−C2	1.515	1.504
C2−C3	1.381	1.408
C3−C4	1.381	1.389
C4−C5		1.402
C3−H	1.108	1.086
	Bond Angle (deg)	
Zn−O1−Zn		109.5
O1−Zn−O2		111.6
O2−Zn−O2		107.3
Zn−O2−C1	130.7	130.7
O2−C1−O2	127.2	126.1
O2−C1−C2	116.4	117.0
C1−C2−C3	120.1	120.2
	Dihedral Angle (deg)	
O1−Zn−O2−C1	0	0
O2−C1−C2−C3	180	180
C2−C3−C4−C5	0	0

reported values.[48,49] In particular, the dihedral angles O1−Zn−O2−C1, O2−C1−C2−C3, and C2−C3−C4−C5 in the ground state are 0°, 180°, and 0°, respectively. This shows excellent coplanarity between the benzene and six-membered rings consisting of zinc, oxygen, and carbon, depicted in Figure 1b.

The IR spectrum of the ground state for the MOF-5 fragment was calculated using the relativistic DFT method. Comparison of calculated and reported IR spectral values, given in Table 2, enables us to investigate the stretching vibrational

Table 2. Comparison of Our Calculated Vibrational Frequencies with the Experimental Results of MOF-5 in the Ground State

frequency (cm^{-1})		
exptl/ DFT[a,b]	this work	assignment
−252.7[a]	261	central Zn−O stretch
−/470.7[a]	479	peripheral Zn−O stretch
846/840[b]	822	organic benzene ring stretching + in-plane OCO bending of the carboxylate group
1615/1603[b]	1576	organic benzene ring breathing

[a]Reference 39. [b]Reference 24.

frequencies of the Zn−O1 and Zn−O2 bonds, organic benzene ring stretching and breathing, as well as in-plane OCO bending of carboxylate group. The calculated vibrational frequencies are in good agreement with the reported value.[30,48]

We calculated the UV−vis spectra of the MOF-5 fragment and free H_2BDC ligand, as shown in Figure 2. The spectra feature one intense absorption at 349 nm and are good agreement with the experimental results (350 nm).[21] The free H_2BDC ligand exhibits an intense absorption at 327 nm. Because the absorption peak of MOF-5 is similar to that of the free H_2BDC ligand, we should assign it to the interligand electronic transition of the H_2BDC ligand. Therefore, these

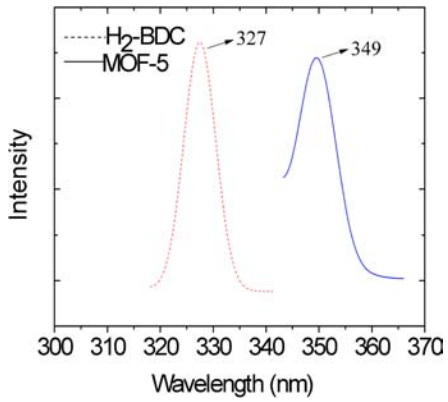

Figure 2. Comparison of the UV−vis absorption spectra of MOF-5 (solid lines) and the free H_2BDC ligand (dashed lines).

results for the ground state, IR spectra, and UV−vis spectra show that the truncated MOF-5 fragment reproduces reliably the experimental results.

Frontier MOs and the Electronic Configuration. In previous reports, the luminescent mechanism in MOF-5 was investigated mostly from electronic absorption and emission spectra.[19−21] However, having not been confirmed, this merits a thorough investigation. In this work, we studied charge transfer associated with MOF-5 luminescence using frontier MOs and the electronic configuration. Kasha's rule states, in principle, that photon emission (fluorescence or phosphorescence) occurs in appreciable yields only from the lowest excited state of a given multiplicity (S_1 and T_1). Generally, emissions originate from the lowest unoccupied molecular orbital (LUMO) to the highest occupied molecular orbital (HOMO). The frontier MOs can also play a critical role in the emission process and influence luminescence. We calculated frontier MOs and the electronic configuration of the MOF-5. From the frontier MOs illustrated in Figure 3b, one can find that the HOMO and LUMO orbitals have carbon atom π and π^* character, respectively. Therefore, it is evident that the S_1 state has $\pi\pi^*$ character. A further observation indicates that the electron densities of the HOMO singlet state are about located in the carbon atoms of the six BDC^{2-} ligands, whereas the densities for the LUMO are distributed mainly about the carbon atoms in only four BDC^{2-} ligands. Thus, the transition from LUMO to HOMO involves the interligand charge transfer. Moreover, from the electronic configuration of the MOF-5 fragment as shown in Figure 3a, the electronic emission from LUMO to HOMO is mainly provided by the carbon atoms because LUMO−HOMO transitions involve interligand charge transfer. The contribution of carbon atoms to HOMO is 93.8%, and those of carbon and oxygen atoms to LUMO are 70.43% and 18.1%, respectively. However, the zinc contributions to HOMO and LUMO are both 0%. Generally, LLCT corresponds to the electronic transition from an organic linker-localized orbital to another organic linker-localized orbital, while LMCT corresponds to the electronic transition from an organic linker-localized orbital to a metal-centered orbital.[10,11] Therefore, this suggests that the emission observed in MOF-5 originates exclusively from the LLCT rather than from the Zn_4O QDs or the based ligand.

Behavior of MOF-5 in the Electronically Excited State. We calculated the geometry, bond order, and IR spectrum of the excited state for MOF-5 using the relativistic TDDFT method and compared these with those of the ground state.

dx.doi.org/10.1021/ic301771b | Inorg. Chem. 2012, 51, 12389−12394

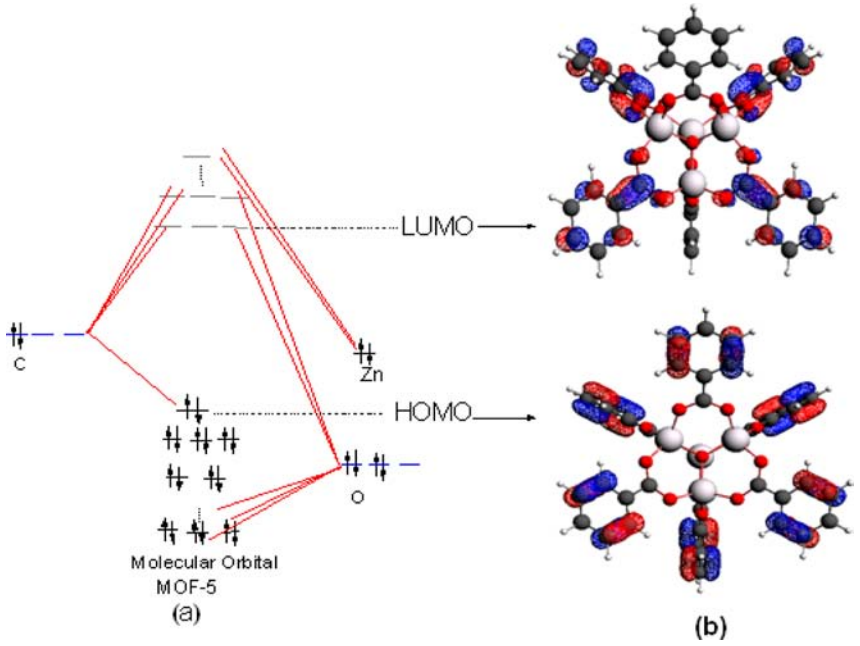

Figure 3. Electron configuration and frontier MOs of MOF-5.

Meanwhile, we also calculated the emission spectra of MOF-5 and the ligand H_2BDC, which reveal the origin of MOF-5 luminescence.

i. Geometry and Emission Spectra in the Electronically Excited State. The geometric parameters of the ground and excited states are listed in Table 3, which indicates that the coordination bonds O1−Zn and O2−Zn are unchanged for the excited state. The bonds O2−C1, C2−C3, C3−C4, and C4−C5 in the ligand BDC^{2-} have a different degrees of weakening in this transition, but the C1−C2 bond has been strengthened. The Zn−O1−Zn and O1−Zn−O2 bond angles are also nearly unchanged in this transition, although the bond angle C1−C2−C3 is increased by 0.5° from the S_0 to the S_1 state. Therefore, the benzene ring in the excited state shows expansion, whereas the Zn_4O_{13} QDs are completely rigid. In addition, the dihedral angles O1−Zn−O2−C1, O2−C1−C2−C3, and C2−C3−C4−C5 are 0°, 180°, and 0°, respectively, for both the ground and electronic excited states. This shows that the six-membered ring of Zn−O−C and the benzene ring are forming a strong coplanarity structure, as depicted in Figure 1b.

Table 3. Bond Length (Å), Bond Angle (deg), and Dihedral Angle (deg) for MOF-5 in S_0 and S_1

	MOF-5	
parameter	S_0	S_1
	Bond Length (Å)	
O1−Zn	1.978 (0.2866)	1.978 (0.2869)
O2−Zn	1.987 (0.2927)	1.987 (0.9320)
O2−C1	1.284 (1.3501)	1.289 (1.3474)
C1−C2	1.504 (1.0178)	1.495 (1.0248)
C2−C3	1.408 (1.3727)	1.411 (1.3711)
C3−C4	1.398 (1.4480)	1.405 (1.4478)
C4−C5	1.402 (1.4257)	1.403 (1.4264)
	Bond Angle (deg)	
Zn−O1−Zn	109.5	109.5
O1−Zn−O2	111.6	111.7
O2−Zn−O2	107.3	107.1
Zn−O2−C1	130.7	130.4
O2−C1−O2	126.1	126.2
O2−C1−C2	117.0	116.9
C1−C2−C3	120.2	120.7
	Dihedral Angle (deg)	
O1−Zn−O2−C1	0	0
O2−C1−C2−C3	180	180
C2−C3−C4−C5	0	0

The calculated emission spectra for MOF-5 and H_2BDC are shown in Figure 4. MOF-5 and H_2BDC exhibit significant emissions at 390 and 350 nm, respectively. Although the emission for high-purity MOF-5 was observed at 397 nm by Feng et al.,[21] the calculated results from the relativistic TDDFT method are in good agreement with this experimental value, thereby giving credible support to the MOF-5 geometry corresponding to the excited state. The emission for MOF-5 is similar to that for H_2BDC but not for the ZnO QD at 560 nm. This reveals that MOF-5 luminescence is possibly linked with the ligand H_2BDC rather than the ZnO QD.

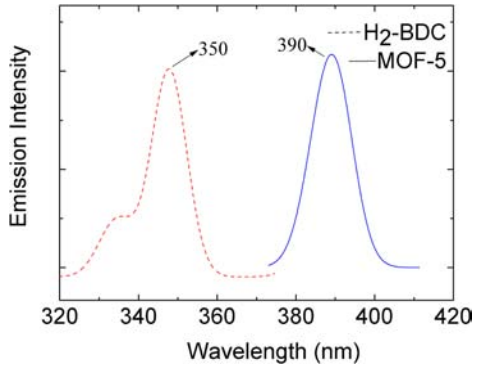

Figure 4. Comparison of the emission spectra for MOF-5 (solid lines) and the free H_2BDC ligand (dashed lines).

ii. Bond Order. The bond orders for MOF-5 in the ground and electronically excited states are listed in parentheses in

dx.doi.org/10.1021/ic301771b | Inorg. Chem. 2012, 51, 12389−12394

Table 3. The bond orders for the Zn−O1 and Zn−O2 bonds are found to be nearly unchanged in the excited state compared to those in the ground state, whereas changes in the bond orders for some bonds in the ligand are consistent with changes in the bond lengths.

iii. IR Spectra. The MOF-5 IR spectra for the ground and excited states (Figure 5) indicate that the vibrational stretching

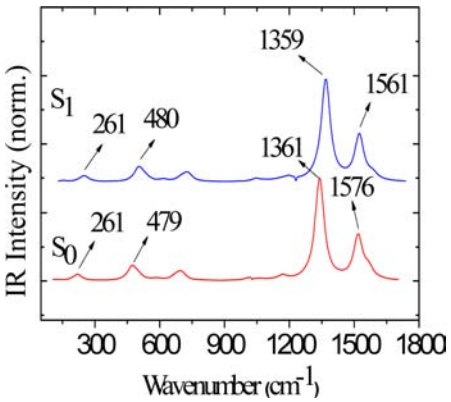

Figure 5. Calculated MOF-5 vibrational absorption spectra for S_0 (red lines) and S_1 (blue lines). The vibrational frequencies of the benzene ring breathing mode in S_0 and S_1 are at 1576 and 1561 cm^{-1}, respectively.

mode frequencies for the Zn−O1 and Zn−O2 bonds are completely unchanged in the excited state. The vibrational breathing mode frequency of the benzene ring is slightly blue-shifted by 15 cm^{-1} from the ground state to the excited state. This result shows that the interaction between each atom in the benzene ring is weakened in the excited state, whereas that of Zn−O remains unchanged. The above calculated result is consistent with the changes in the bond lengths and bond orders for MOF-5 in the excited state.

The above behaviors in the geometry, bond order, and IR spectrum in the excited state combined with the luminescence mechanism show that the BDC^{2-} moiety has been electronically excited to the S_1 state. Thus, the MOF-5 emission should be attributed to LLCT rather than to LMCT. The Zn_4O_{13} QD in the excited state was rigid, which further supports the notion that MOF-5 luminescence does not involve the QDs. The dihedral angle indicates that the six-membered Zn−O−C ring is coplanar with the benzene ring in both the ground and excited states. Generally, luminescence yields benefit from higher molecular rigidity and planarity, which increase the π-electron conjugation and reduce the rate of nonradiative processes, such as internal thermal conversion, intersystem crossover, and molecular vibration.[50−55] This is why MOF-5 exhibits good luminescence.

CONCLUSIONS

We have presented a detailed investigation of the electronically excited state and MOF-5 luminescence using the relativistic DFT and TDDFT. The following important conclusions are obtained: (1) The calculated results for the ground-state geometry, IR spectra, and UV−visible spectroscopy show that the truncated representative segment from the MOF-5 cell used in this investigation provided reasonable quantitative values. Meanwhile, the calculated results, which agree well with the experimental values, show that the relativistic DFT and TDDFT for calculation of MOF-5 are reasonable. (2) The calculated frontier MOs and electronic configuration indicated that the mechanism underlying MOF-5 luminescence originated within neither the ZnO-like QD nor the ligand but from LLCT. (3) Comparing the geometry and IR spectra of both the ground and excited states indicated that the Zn_4O_{13} QD is rigid but the BDC ligands are nonrigid. The MOF-5 emission spectrum is similar to that of H_2BDC but significantly different from that of the ZnO QD, revealing that luminescence is related to the ligand rather than the QD. This finding further proved that the origin of MOF-5 luminescence is LLCT. Thus, the combination of the MOF-5 excited-state behavior and its luminescence mechanism overturns previous reports that the MOF-5 luminescence mechanism is LMCT or ligand-based. (4) The reason for MOF-5 luminescence is that the benzene and six-membered Zn−O−C rings in the ground and excited states have excellent coplanarity. (5) These findings clarify the relationship between the MOF structure and luminescence and may lead researchers to synthesize MOFs of higher luminescence efficiency.

AUTHOR INFORMATION

Corresponding Author

*E-mail: haoce@dlut.edu.cn. Tel.: +86-411-84706323. Fax: +86-411-84748086.

Notes

The authors declare no competing financial interest.

ACKNOWLEDGMENTS

Support of this work by the National Natural Science Foundation of China (Grants 21036006, 21137001, and 21076031) and the Fundamental Research Funds for the Central Universities (Grant DUT12ZD219) is gratefully acknowledged.

REFERENCES

(1) Kupper, R. J.; Timmons, D. J.; Fang, Q. R.; Li, J. R.; Makal, T. A.; Young, M. D.; Yuan, D. Q.; Zhao, D.; Zhuang, W. J.; Zhou, H. C. *Coord. Chem. Rev.* **2009**, *253*, 3042−3066.
(2) Li, J. R.; Kupper, R. J.; Zhou, H. C. *Chem. Soc. Rev.* **2009**, *38*, 1477−1504.
(3) Duren, T.; Baeand, Y. S.; Snurr, R. Q. *Chem. Soc. Rev.* **2009**, *38*, 1237−1247.
(4) Han, S. S.; Mendoza-Cortés, J. L.; Goddard, W. A., III. *Chem. Soc. Rev.* **2009**, *38*, 1460−1476.
(5) Chen, B. L.; Xiang, S. C.; Qian, G. D. *Acc. Chem. Res.* **2010**, *43*, 1115−1124.
(6) Cui, Y. J.; Yue, Y. F.; Qian, G. D.; Chen, B. L. *Chem. Rev.* **2012**, *112*, 1126−1162.
(7) Huang, Y. Q.; Ding, B.; Song, H. B.; Zhao, B.; Ren, P.; Cheng, P.; Wang, H. G.; Liao, D. Z.; Yan, S. P. *Chem. Commun.* **2006**, 4906−4908.
(8) Gunning, N. S.; Cahill, C. L. *Dalton Trans.* **2005**, 2788−2792.
(9) Fang, Q. R.; Zhu, G. S.; Shi, X.; Wu, G.; Tian, G.; Wang, R. W.; Qiu, S. L. *J. Solid State Chem.* **2004**, *177*, 1060−1066.
(10) Zhao, G. J.; Han, K. L.; Stang, P. J. *J. Chem. Theory Comput.* **2009**, *5*, 1955−1958.
(11) Zhao, G. J.; Northrop, B. H.; Han, K. L.; Stang, P. J. *J. Phys. Chem. A* **2010**, *114*, 9007−9013.
(12) Taylor, K. M. L.; Rieter, W. J.; Lin, W. *J. Am. Chem. Soc.* **2008**, *130*, 14358−14359.
(13) Allendorf, M. D.; Bauer, C. A.; Bhakta, R. K.; Houk, R. J. T. *Chem. Soc. Rev.* **2009**, *38*, 1330−1352.
(14) Harbuzaru, B. V.; Corma, A.; Rey, F.; Jordá, J. L.; Ananias, D.; Carlos, L. D.; Rocha, J. *Angew. Chem., Int. Ed.* **2009**, *48*, 6476−6479.

(15) Amouri, H.; Desmarets, C.; Moussa, J. *Chem. Rev.* **2011**, DOI: /10.1021/cr200345v.
(16) Li, H. L.; Eddaoudi, M.; O'Keeffe, M.; Yaghi, O. M. *Nature* **1999**, *402*, 276−279.
(17) Mueller, T.; Ceder, G. *J. Phys. Chem. B* **2005**, *109*, 17974−17983.
(18) Bordiga, S.; Vitillo, J. G.; Ricchiardi, G.; Regli, L.; Cocina, D.; Zecchina, A.; Arstad, B.; Bjørgen, M.; Hafizovic, J.; Lillerud, K. P. *J. Phys. Chem. B* **2005**, *109*, 18237−18242.
(19) Bordiga, S.; Lamberti, C.; Ricchiardi, G.; Regli, L.; Bonino, F.; Damin, A.; Lillerud, K. P.; Bjorgen, M.; Zecchina, A. *Chem.Commun.* **2004**, 2300−2301.
(20) Tachikawa, T.; Choi, J. R.; Fujitsuka, M.; Majima, T. *J. Phys. Chem. C* **2008**, *112*, 14090−14101.
(21) Feng, P. L.; Perry, J. J., IV; Nikodemski, S.; Jacobs, B. W.; Meek, S. T.; Allendorf, M. D. *J. Am. Chem. Soc.* **2010**, *132*, 15487−15489.
(22) Ameloot, R.; Roeffaers, M. B. J.; Cremer, G.; De Vermoortele, F.; Hofkens, J.; Sels, B. F.; De Vos, D. E. *Adv. Mater.* **2011**, *23*, 1788−1791.
(23) Khajavi, H.; Gascon, J.; Schins, J. M.; Siebbeles, L. D. A.; Kapteijn, F. *J. Phys. Chem. C* **2011**, *115*, 12487−12493.
(24) Gehlen, M. H.; De Schryver, F. C. *Chem. Rev.* **1993**, *97*, 11242−11248.
(25) Zhao, G. J.; Han, K. L.; Lei, Y. B.; Dou, Y. *J. Chem. Phys.* **2007**, *127*, 094307-1−094307-6.
(26) Han, K. L.; He, G. Z. *J. Photochem. Photobiol. C: Photochem. Rev.* **2007**, *8*, 55−66.
(27) Zhao, G. J.; Northrop, B. H.; Stang, P. J.; Han, K. L. *J. Phys. Chem. A* **2010**, *114*, 3418−3422.
(28) Zhao, G. J.; Yu, F. B.; Zhang, M. X.; Northrop, B. H.; Yang, H. B.; Han, K. L.; Stang, P. J. *J. Phys. Chem. A* **2011**, *115*, 6390−6393.
(29) Zhao, G. J.; Han, K. L. *Acc. Chem. Res.* **2012**, *45*, 404−413.
(30) Hu, Y. H.; Zhang, L. *Phys. Rev. B* **2010**, *81*, 174102-1−174102-6.
(31) Yang, L. M.; Vajeeston, P.; Ravindran, P.; Fjellvag, H.; Tilset, M. *Inorg. Chem.* **2010**, *49*, 10283−10290.
(32) Petrov, T.; Michalkova, A.; Leszczynski, J. *Struct. Chem.* **2010**, *21*, 391−404.
(33) Beeke, A. D. *J. Chem. Phys.* **1993**, *98*, 5648−5652.
(34) Perdew, J. P.; Burke, K. *Phys. Rev. Lett.* **1997**, *78*, 1396−1396.
(35) Lee, C.; Yang, W.; Parr, R. G. *J. Phys. Rev. B* **1988**, *37*, 785−789.
(36) Dunning, T. H., Jr.; Hay, P. J. *Methods of Electronic Structure Theory [C]*; Plenum: New York, 1977.
(37) Pyykko, P. *Chem. Rev.* **1988**, *88*, 563−594.
(38) Shamov, G. A.; Schreckenbach, G.; Martin, R. L.; Hay, P. J. *Inorg. Chem.* **2008**, *47*, 1465.
(39) van Lenthe, E.; van Leeuwen, R.; Baerends, E. J. *Int. J. Quantum Chem.* **1996**, *57*, 281−293.
(40) van Lenthe, E.; Ehlers, A. E.; Baerends, E. J. *J. Chem. Phys.* **1999**, *110*, 8943−8953.
(41) Laikov, D. N. An Implementation of the Scalar Relativistic Density Functional Theory for Molecular Calculations with Gaussian Basis Sets. DFT2000 Conference, Menton, France, 2000.
(42) Shamov, G. A. *Inorg. Chem.* **2012**, *51*, 6507−6516.
(43) Kamya, P. R. N.; Muchall, H. M. *J. Phys. Chem. A* **2011**, *115*, 12800−12808.
(44) Wong, B. M.; Piacenzab, M.; Sala, F. D. *Phys. Chem. Chem. Phys.* **2009**, *11*, 4498−4508.
(45) Nakata, A.; Tsuneda, T.; Hirao, K. *J. Chem. Phys.* **2011**, *135*, 224106−1−9.
(46) Te Velde, G.; Bickelhaupt, F. M.; Baerends, E. J. *J. Comput. Chem.* **2001**, *22*, 931−967.
(47) Guerra, C. F.; Snijders, J. G.; te Velde, G.; Baerends, E. J. *Theor. Chem. Acc.* **1998**, *99*, 391−403.
(48) Civalleri, B.; Napoli, F.; Roetti, C.; Roetti, C.; Doves, R. *CrystEngComm* **2006**, *8*, 368−371.
(49) Yildirim, T.; Hartman, M. R. *Phys. Rev. Lett.* **2005**, *95*, 2155040−1−8.
(50) Lakowicz, J. R. Principles of Fluorescence Spectroscopy, 2nd ed.; Kluwer Academic: New York, 1999.
(51) Valeur, B. *Molecular Fluorescence: Principles and Applications*; Wiley-VCH Verlag: Weinheim, Germany, 2001.
(52) Zhao, G. J.; Han, K. L. *J. Phys. Chem. A* **2007**, *111*, 9218−9223.
(53) Zhao, G. J.; Liu, J. Y.; Zhou, L. C.; Han, K. L. *J. Phys. Chem. B* **2007**, *111*, 8940−8945.
(54) Zhao, G. J.; Han, K. L. *Biophys. J.* **2008**, *94*, 38−46.
(55) Zhao, G. J.; Han, K. L. *ChemPhysChem* **2008**, *9*, 1842−1846.